Aspects of Multidimensional Upwinding: Time-Dependent Nonlinear Systems, Source Terms, Spherical Geometries and Three-Dimensional Grid Adaptation. *

M.E.Hubbard

The University of Reading, Department of Mathematics,

P.O.Box 220, Whiteknights, Reading, Berkshire, RG6 6AX, U.K.

30th June 1999

*This work has been carried out as part of the Oxford/Reading Institute for Computational Fluid Dynamics and was funded by EPSRC.

Abstract

A number of peripheral aspects relating to the application of multidimensional upwind schemes in new areas are presented, expanding on their current capabilities. In summary: 1) recently developed high order schemes for the scalar advection equation are applied to nonlinear systems of equations, 2) source term decompositions are presented which are appropriate to existing wave models, 3) the two-dimensional scalar fluctuation distribution schemes are modified for flow over curved surfaces, in particular on the sphere, 4) a simple node movement algorithm (used previously in two dimensions) is applied to steady state solutions of the three-dimensional scalar advection equation.

1 Introduction

This report has been written to summarise the current state of a number of strands of research associated with the application of multidimensional upwind schemes (see [6] for full details of these methods) to a wider range of problems. It is divided into four short sections:-

2. Multidimensional upwinding has now matured to a stage where it is being used in practical situations for the modelling of steady state aerodynamic problems [9]. However, there is still much work to be done for the approximation of time-dependent flows. Advances have been made for the scalar advection equation [4], combining high order schemes with genuinely multidimensional limiting procedures, and here these techniques are applied to nonlinear systems via existing decompositions. It is clear from the results that although the accuracy is improved significantly there is a necessity for the construction of new and improved wave models.

3. Source terms prove to be relatively straightforward to include as part of the fluctuation distribution algorithm and, with the exception of the simple wave models, they can be extended simply to be incorporated within system decompositions. The general technique is described here and compared with the commonly used pointwise approach to illustrate the improvement. In the case of simple wave models one possible method of decomposing and discretising the source terms is described, but it is complicated and unclear as to whether it gives any improvement over the much simpler pointwise discretisation.

4. In meteorological flows the shallow water equations are often modelled on the sphere. The decomposition stage of the multidimensional upwind algorithm is not straightforward in this situation, but the scalar schemes can be applied on spherical geometries with little difficulty (if conservation is not enforced) and the method is presented here.

5. The grid movement algorithm applied successfully in two dimensions in [1] generalises easily to three dimensions and is applied here to simple scalar

advection test cases to illustrate its effectiveness.

2 Time Dependent Nonlinear Systems

The extension of the time-dependent fluctuation redistribution schemes of [4] to nonlinear systems of equations is relatively straightforward and follows closely that of the finite element method [10]. Given that the flux balance can be split up into scalar components, the process differs little from the scalar case:

- compute the low and high order element contributions to the grid nodes using the PSI and Lax-Wendroff schemes respectively, then use these to construct the antidiffusive element contributions (AEC's), storing not only the AEC's for each wave in the decomposition (in the form of distribution coefficients and fluctuations) but also the accumulated element contributions (for speed in calculating the appropriate bounds on the updated solution and hence the required limiting factors).

- compute the complete low order update and use this to obtain bounds on the solution at the new time level.

- use these bounds to calculate limiting factors on the antidiffusive element contributions. These bounds are necessarily constructed from the original solution and the overall updates in terms of the conservative variables. This is because it is not possible to convert perturbations in the conservative variables into perturbations of the 'characteristic' variables associated with the individual waves in the decomposition (due either to the presence of source terms in the decomposition or the linear dependence of the components, depending on the type of wave model used). As a consequence, each wave in the decomposition utilises the same limiting factor at a given cell vertex. This may be based solely on one variable (*e.g.* density for the Euler equations, depth for the shallow water equations) or taken to be a minimum of the limiting factors over a set of independent variables, such as all of the conservative variables (which should minimise the oscillations in the solution).

- apply the limiting factors to each wave in turn (it was noted in [10] that it is not desirable to use separate limiting factors on each equation even though this would be less diffusive), transforming the distribution coefficients via the fluctuation redistribution approach of [4], for which only the low and high order distribution coefficients and the limiting factors are required *a priori*.

  Note that flux-corrected transport can be applied without reference to the decomposition. A single limiting factor is calculated for the cell whichever vertex is considered and this can be applied directly to the overall updates (a quicker but slightly less accurate method).

- use the new distribution coefficients to update the solution in the manner of the standard fluctuation distribution algorithm.

2.1 Results

Results are shown here for two one-dimensional test cases, both approximated on the two-dimensional grid shown in Figure 2.1 before the solutions are averaged over the breadth of the computational domain, $[-50, 50] \times [0, 10]$, to allow comparison to be made with exact one-dimensional solutions. For the Euler equations, the well known Sod shock tube problem is used in which a gas is initially at rest and the flow evolves from two constant states on either side of a given position, taken here to be $x = 0.0$. The two states are related by a density ratio of 1:8 and a pressure ratio of 1:10 between the right and left solution values. For the shallow water equations the analogous problem is presented: the dam break problem, here with a depth ratio of 1:10. Figures 2.2 and 2.3 show the comparison between the low order results obtained using Roe's model D and Rudgyard's Mach angle splitting as wave models and the results obtained when the fluctuation redistribution is applied to each of the scalar components of the decomposition. A small improvement in accuracy is apparent but oscillations are not completely removed. Roe's model D did not prove to be very robust, particularly for transcritical cases. The Mach/Froude angle splitting had fewer difficulties, which allowed much larger differences to be taken between the left

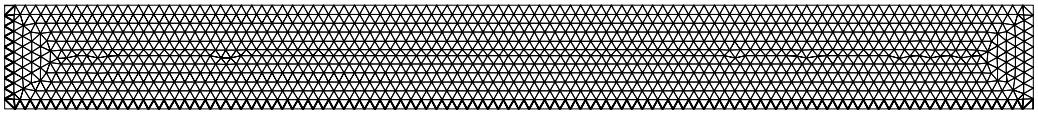

Figure 2.1: The computational grid.

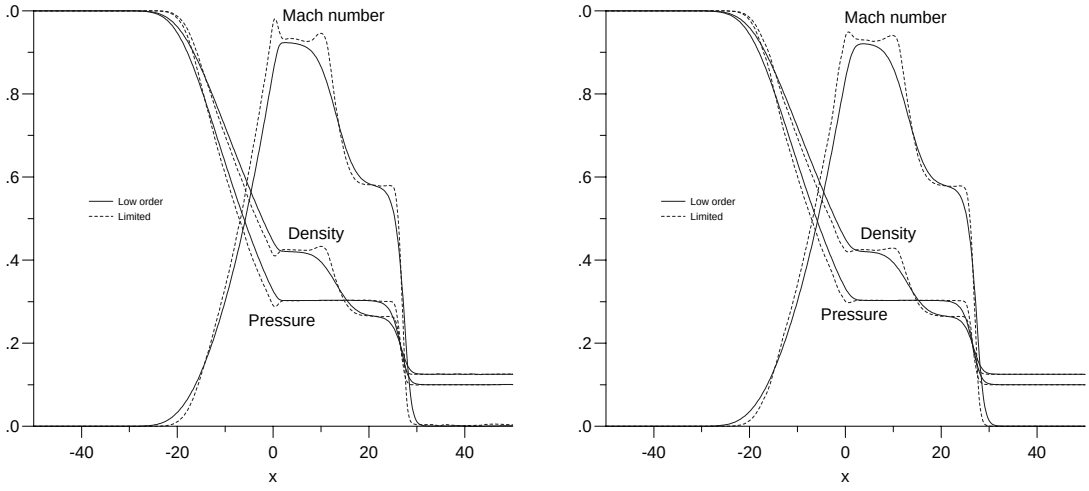

Figure 2.2: Breadth-averaged two-dimensional solutions for Sod's shock tube using Model D (left) and the Mach angle splitting (right).

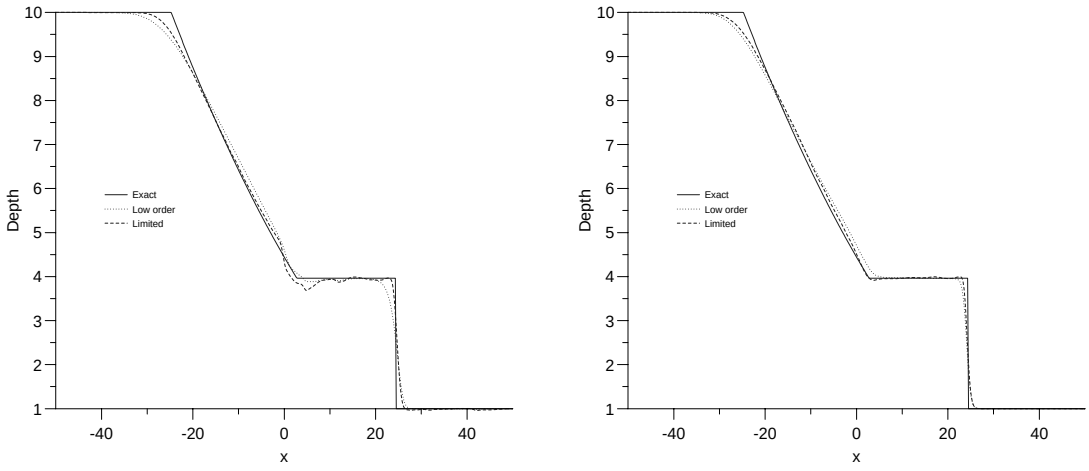

Figure 2.3: Breadth-averaged two-dimensional solutions for a dam break problem using Model D (left) and the Mach angle splitting (right).

and right states before the scheme produced unphysical solutions. Note though that this problem could be alleviated to some extent by increasing the diffusive component of the Lax-Wendroff scheme.

The techniques were also applied to the approximate diagonalisation methods, with similar success but an even more significant lack of robustness, mainly due to the fact that the coupling terms inherent in these models destroy the concept of positivity which is used in the construction of the distribution schemes. Unfortunately, due to their singular nature at stagnation points it is not feasible to apply the preconditioned decompositions even in these simple cases.

3 Source Terms

In two dimensions, source terms have been included in the systems of conservation laws which have been modelled, so the equations become

$$\underline{U}_t + \underline{F}_x + \underline{G}_y \;=\; \underline{S}\,, \tag{3.1}$$

$\underline{U}$ being the vector of conservative variables, $\underline{F}$ and $\underline{G}$ the conservative fluxes and $\underline{S}$ containing the source terms. The obvious way to include the source term within the approximation is to evaluate over the triangular cell, in place of the flux balance, the quantity

$$\underline{\Phi} \;=\; -\int\!\!\int (\underline{F}_x + \underline{G}_y - \underline{S})\,\mathrm{d}x\,\mathrm{d}y\,. \tag{3.2}$$

In this way the sources simply augment the existing terms which appear either because of the linearisation or the decomposition [8, 2] and the form of the final scheme is unchanged, only the definitions of the fluctuations ϕ. The augmented sources can then be dealt with in a manner which takes into account the type of wave model used:

- **Simple wave models**: the source term is split into x- and y-components so that the system can be written

$$\underline{U}_t + \mathbf{A}(\underline{U}_x - \mathbf{A}^{-1}\underline{S}^x) + \mathbf{B}(\underline{U}_y - \mathbf{B}^{-1}\underline{S}^y) \;=\; \underline{0} \tag{3.3}$$

  as long as $\mathbf{A}$ and $\mathbf{B}$, the conservative flux Jacobians, are invertible, or equivalently

$$\underline{U}_t + (\mathbf{A},\mathbf{B})\cdot\vec{\nabla}\underline{U}^\delta \;=\; \underline{0} \tag{3.4}$$

which contains a perturbed gradient of the conservative variables, given by

$$\vec{\nabla}\underline{U}^{\delta} \;=\; (\underline{U}_x - \mathbf{A}^{-1}\underline{S}^x, \underline{U}_y - \mathbf{B}^{-1}\underline{S}^y)^{\mathrm{T}}\,. \tag{3.5}$$

It is this quantity which can now be decomposed into components due to gradients of plane wave solutions to the nonlinear system, *i.e.*

$$\vec{\nabla}\underline{U}^{\delta} \;=\; \sum_{k=1}^{N_w} \varphi^k\, \underline{r}^k\, (\vec{n}_\theta)^{\mathrm{T}} \tag{3.6}$$

and this equation is solved for the specified wave strengths φ and propagation directions θ associated with the chosen wave model. ($\underline{r}$ are eigenvectors of the matrix $(\mathbf{A},\mathbf{B})\cdot\vec{n}_\theta$ appropriate to the chosen waves and $\vec{n}_\theta$ is a unit vector with orientation θ.) Each component of (3.6) relates to a scalar fluctuation which can be incorporated into a distribution scheme in the usual way.

- **Characteristic decompositions**: the source term is decomposed using the same similarity transformation as is used on the rest of the system. In 'characteristic' variables $\underline{W}$ the equations are

$$\underline{W}_t + \mathbf{A}_{\mathrm{W}}\underline{W}_x + \mathbf{B}_{\mathrm{W}}\underline{W}_y \;=\; \underline{S}_{\mathrm{W}}\,, \tag{3.7}$$

in which $\underline{S}_{\mathrm{W}} = \frac{\partial \underline{U}}{\partial \underline{W}}^{-1}\underline{S}$. This leads to a number of scalar 'advection' equations of the form

$$W_t + \vec{\lambda}\cdot\vec{\nabla}W + q \;=\; S_{\mathrm{W}}\,, \tag{3.8}$$

each of which has its own advection velocity $\vec{\lambda}$ and coupling term q, and subsequently a flux balance which includes the source term, *i.e.*

$$\underline{\Phi} \;=\; -S_\triangle \sum_{k=1}^{N_w} (\vec{\lambda}^k\cdot\vec{\nabla}W^k + q^k - S^k_{\mathrm{W}})\underline{r}^k\,, \tag{3.9}$$

where $\underline{r}$ are the columns of the transformation matrix $\frac{\partial \underline{U}}{\partial \underline{W}}$. The distribution coefficients are calculated as though for the homogeneous equations and then applied to the above fluctuations,

$$\phi^k \;=\; -S_\triangle(\vec{\lambda}^k\cdot\vec{\nabla}W^k + q^k - S^k_{\mathrm{W}})\,, \tag{3.10}$$

before calculating the conservative updates.

- **Preconditioned decompositions**: the source term is decomposed in the same way as in the characteristic decomposition above except that the preconditioner is introduced into the transformation, so the flux balance again has the form

$$\underline{\Phi} \;=\; -S_{\triangle} \sum_{k=1}^{N_w} (\vec{\lambda}^k \cdot \vec{\nabla} W^k + q^k - S^k_{\rm W}) \underline{r}^k \; . \tag{3.11}$$

but $\underline{r}$ are now the columns of the matrix $\frac{\partial \underline{\underline{U}}}{\partial \underline{\underline{Q}}} \mathbf{P}^{-1} \frac{\partial \underline{\underline{Q}}}{\partial \underline{\underline{W}}}$ and $\underline{S}_W = \frac{\partial \underline{\underline{W}}}{\partial \underline{\underline{Q}}} \mathbf{P} \frac{\partial \underline{\underline{Q}}}{\partial \underline{\underline{U}}} \underline{S}$. Once more, the solution procedure is no different from the homogeneous case with modified fluctuations.

As an example, the shallow water equations with additional terms for modelling bed slope are solved combining the above technique with the hyperbolic/elliptic preconditioned decomposition adapted from that of Mesaros and Roe [12], and described in detail in [8]. The source terms considered here are

$$\underline{S} \;=\; \begin{pmatrix} 0 \\ gdh_x \\ gdh_y \end{pmatrix} \;=\; \begin{pmatrix} 0 \\ S_X \\ S_Y \end{pmatrix} \tag{3.12}$$

where d is depth, h is depth below still water and g is the acceleration due to gravity, and which, when the transformation to characteristic variables is applied, becomes

$$\underline{S}_W \;=\; \frac{1}{q^2 d} \begin{pmatrix} -\varepsilon u S_X - \varepsilon v S_Y \\ -\beta v S_X + \beta u S_Y \\ \varepsilon F u S_X + \varepsilon F v S_Y \end{pmatrix} \tag{3.13}$$

in subcritical flow and

$$\underline{S}_W \;=\; \frac{1}{q^2 d} \begin{pmatrix} -(u + \beta v) S_X - (v - \beta u) S_Y \\ -(u - \beta v) S_X - (v + \beta u) S_Y \\ F u S_X + F v S_Y \end{pmatrix} \tag{3.14}$$

when the flow is supercritical. As in [8], u and v are the two velocity components, $q = \sqrt{u^2 + v^2}$ is the flow speed, $F = q/\sqrt{gd}$ is the local Froude number,

$$\beta \;=\; \sqrt{|F^2 - 1|} \quad , \qquad \kappa \;=\; \max(F, 1) \; , \tag{3.15}$$

and, in this case, ε is taken to be

$$\varepsilon(F) \;=\; \begin{cases} -F^3 + \frac{3}{2}F^2 + \frac{1}{2} & \text{for} \quad 0 \;\leq\; F \;\leq\; 1 \\ 1 & \text{for} \quad F \;>\; 1\,. \end{cases} \tag{3.16}$$

3.1 Results

Results are shown, comparing the upwind distribution of the source terms described above with a simple pointwise evaluation at each node which is added after the fluctuation distribution has been carried out. In the multidimensional upwind notation this scheme looks like

$$\underline{U}_i^{n+1} \;=\; \underline{U}_i^n + \frac{\Delta t}{S_i} \sum_{j \in \cup \Delta_i} \sum_{k=1}^{N_w} (\alpha_i^j)^k \phi_j^k \, \underline{r}_j^k + \Delta t \, \underline{S}_i \;. \tag{3.17}$$

This is done for a one-dimensional problem of flow over a smoothly varying symmetric bump in a channel using the grid shown in Figure 3.1 (which gives roughly 75 cells in the streamwise direction). The computational domain is the region $[0,3] \times [0,1]$ and the bathymetry is defined by

$$h(x) \;=\; \begin{cases} 1.0 - z_{\max} \cos^2(\pi(x - 1.5)) & \text{for} \quad |x - 1.5| \;\leq\; 0.5 \\ 1.0 & \text{otherwise}\,, \end{cases} \tag{3.18}$$

in which $z_{\max} = 0.1$ is the maximum height of the bed above the level at inflow. This has been chosen as a simple channel geometry for which exact steady state solutions to the one-dimensional shallow water equations are available for comparison [7] with the breadth-averaged numerical results.

Three flows are compared, defined by:

- $F_\infty = 0.5$, $d_\infty = 1.0$, giving purely subcritical flow which is symmetric about the peak of the bump (at $x = 1.5$),
- $F_\infty = 0.65$, $d_\infty = 1.0$, giving transcritical flow with a stationary hydraulic jump downstream of the peak and a critical point at the peak,
- $F_\infty = 1.4$, $d_\infty = 1.0$, giving purely supercritical flow which is symmetric about the peak.

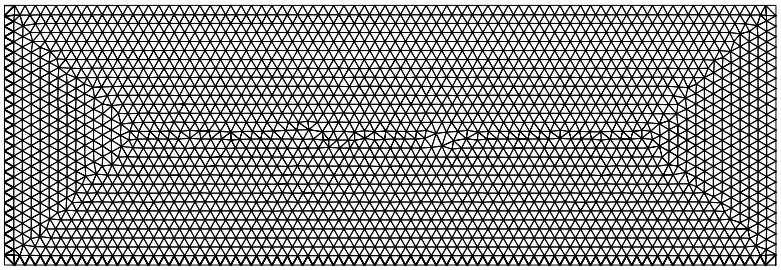

Figure 3.1: The grid for the channel flow with sloping bed.

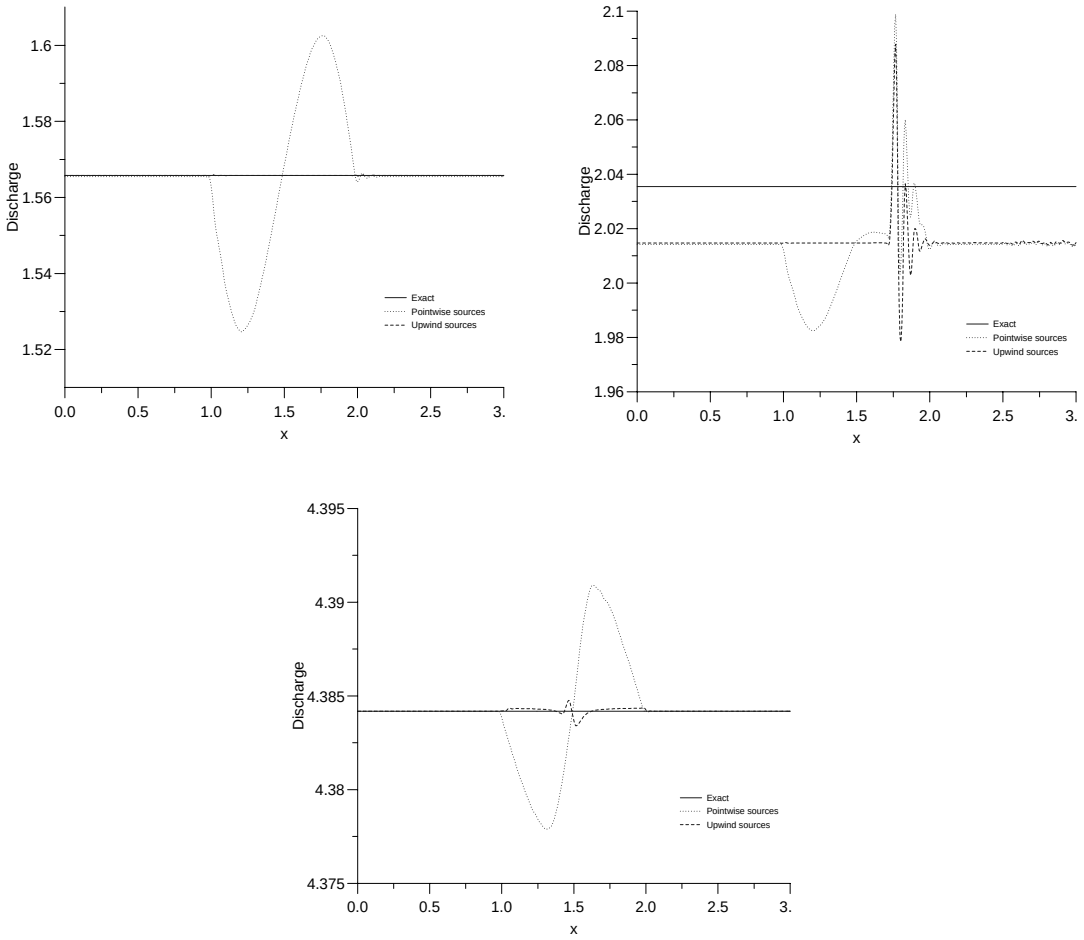

Figure 3.2: Solutions for the symmetric channel with varying bed for $F_\infty = 0.5$ (top left), $F_\infty = 0.65$ (top right) and $F_\infty = 1.4$ (bottom).

The subscript $\cdot_\infty$ represents the freestream flow values 'at infinity' which are used in the application of simple characteristic boundary conditions at inflow and outflow: appropriate Riemann invariants are specified, *cf.* [7].

Each of the sets of results in Figure 3.2 shows an improvement when the upwind discretisation of the source term is used. Discharge is supposed to remain constant throughout the channel for steady state flows. The small discrepancies seen in the supercritical case are there simply due to linearisation errors and could be removed with a little extra effort in the linearisation of the source term to achieve an exact balance with the linearised flux gradients. In the transcritical flow case, the difference from the exact one-dimensional solution appears to come from the application of the boundary conditions in two dimensions, and is visible in results obtained from other forms of numerical scheme.

4 Multidimensional Upwinding on the Sphere

The first question which needs to be addressed here is whether the schemes should be applied in a three-dimensional Cartesian coordinate system or a spherical polar coordinate system. The former has been chosen here because it avoids the singularity which appears at the poles in the latter. Since the schemes are applied on unstructured triangular grids there is no problem with grid singularities, which occur in many existing structured codes. The big advantage of this approach is that the advection is treated in the same way, regardless of position on the surface of the sphere and direction of travel.

Ideally, the underlying scheme would be based on the two-dimensional multidimensional upwind schemes, but applied on a curved surface. Unfortunately, since the divergence theorem can no longer be applied in the conservation argument, the resulting scheme is not conservative because internal cancellation can no longer be guaranteed. However, in the scalar case it should be simple to construct a conservative three-dimensional scheme on a prismatic grid over the surface of the sphere in which the solution is constrained to be constant perpendicular to the curved surface. For the moment, it is noted that the fluctuation in a triangle is independent of the orientation of that triangle in three-dimensional

space so, given a two-dimensional set of orthogonal coordinates ξ and η in the plane of the triangle on the surface, the fluctuation can be defined by

$$\phi \;=\; \int\!\!\int_{\triangle} \vec{\nabla}_{\xi\eta} \cdot (f^{\xi}, g^{\eta})\, \mathrm{d}\xi\, \mathrm{d}\eta\,, \tag{4.1}$$

where f and g are both functions of u. This can be approximated by

$$\tilde{\phi} \;=\; -S_{\triangle} \tilde{\vec{\lambda}}_{\xi\eta} \cdot \vec{\nabla}_{\xi\eta} u \;\approx\; \oint_{\partial\triangle} (f^{\xi}, g^{\eta}) \cdot \mathrm{d}\vec{n}_{\xi\eta}\,. \tag{4.2}$$

Alternatively, in keeping with the three-dimensional coordinate system, one can take

$$\tilde{\phi} \;=\; \sum_{k=1}^{N_e} (\tilde{f}, \tilde{g}, \tilde{h}) \cdot \vec{n}_k \tag{4.3}$$

in which $\vec{n}_k$ is a three-dimensional 'outward' normal to the edge of the triangle whose direction is tangent to the surface at the midpoint of the edge and whose component in the plane of the cell has the same length as the corresponding edge. Thus $\vec{n}_k$ is not in the ξ-η coordinate plane and the approximation cannot be exact, even under the assumptions of linearly varying u and constant advection. However, both of the above approximations are consistent and the distribution coefficients can be calculated as for the two-dimensional scheme (since everything is carried out locally on the triangle) and the same overall update used.

4.1 Results

Figure 4.1 shows the initial conditions (and the exact solution after one revolution) for the advection of a cosine bell around a great circle of a sphere proposed in [13]. Figures 4.2 and 4.3 show the numerical solution on the coarse grid illustrated (1357 nodes, 2710 cells) after one revolution, respectively around the equator and across the poles. The scheme used is in fact the implicit consistent finite element version of the PSI scheme [11] with flux-corrected transport applied to ensure monotonicity and the solutions look reasonably good despite the lack of conservation. Importantly there is little difference between the solutions obtained for the advection over the poles and around the equator, and no special treatment of the poles has been necessary.

Figure 4.1: The initial conditions for advection on the sphere.

Figure 4.2: The solution after one revolution around the equator for advection on the sphere.

Figure 4.3: The solution after one revolution across the poles for advection on the sphere.

5 Three-Dimensional Grid Adaptation

The simple grid movement algorithm of [1] has been applied to the three-dimensional scalar advection equation,

$$u_t + f_x + g_y + h_z \;=\; 0\,, \tag{5.1}$$

to improve the accuracy of the steady state solutions obtained using the PSI fluctuation distribution scheme [5].

The underlying idea is simple: between solution iterations the nodes are moved to a weighted average of the positions of the neighbouring cell centroids, *i.e.*

$$\vec{x}_i^{new} \;=\; \frac{\sum_{j\in \cup\triangle_i} w_j \vec{x}_j}{\sum_{j\in \cup\triangle_i} w_j}\,, \tag{5.2}$$

where the $\vec{x}_j$ are the positions of the centroids, w_j are the cell weights and j indicates the cells adjacent to node i. The weights here are chosen to depend on local approximations to the first and second derivatives of the solution u, so

$$w \;=\; \left(1 + \beta_1 |\vec{\nabla} u|^2 + \beta_2 (\vec{\nabla}^2 u)^2\right)^{1/2}\,, \tag{5.3}$$

where β_1 and β_2 are chosen to improve the final results. Mesh tangling is avoided by artificially limiting the distance which a node can move. A simple but rather restrictive limit is

$$(\Delta x_i)_{\max} \;=\; \frac{3}{2} \min_{j\in \cup C_i} \left(\frac{V_j}{\max_{k=1,4} A_{jk}} \right)\,, \tag{5.4}$$

where V_j is the volume of cell j, A_{jk} is the area of face k of cell j, and the minimum is taken over all cells with a vertex at node i, denoted by $\cup C_i$. A displacement can be found for all nodes, including boundary 'face' and 'edge' nodes which must then be projected back on to the nearest point on corresponding part of the boundary, and 'corner' nodes, even though they are then forced to remain fixed.

The overall solution strategy is expressed by the following three stages:

1) run the time-stepping algorithm on an initial, fixed grid until the solution appears steady (but long before convergence is achieved).

2) run the time-stepping interspersed with the grid movement until the grid has adapted to the steady solution. In this work, each time-step is alternated with a single node movement iteration.

3) fix the grid and run the time-stepping algorithm to convergence using the solution from step 2) as initial conditions.

5.1 Results

Results are shown for a simple test case of advection through a cube with dimensions $[-1,0] \times [0,1] \times [0,1]$, as described in [5]. The boundary conditions are zero everywhere at inflow except on $z = 0$ where $u = 1$ for $r < 1$, where $r^2 = 4(x+0.5)^2 + 5(y-0.35)^2$ (giving an ellipse). The advection velocity is given by

$$\vec{\lambda} = (z,\, 0.25,\, -x)^{\mathrm{T}} \,. \tag{5.5}$$

The grid is constructed from a uniform $21 \times 21 \times 21$ node Cartesian mesh, each cell of which is divided into 5 tetrahedra, as shown in Figure 5.1.

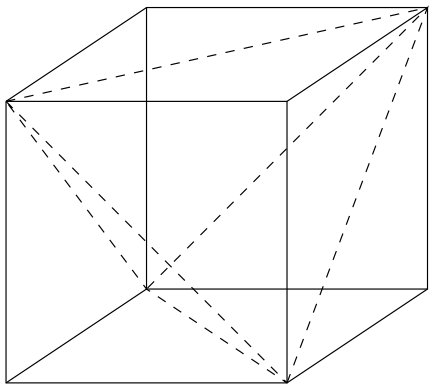

Figure 5.1: The division of a cube into five tetrahedra.

Preliminary results are shown in Figure 5.2, for parameters $\beta_1 = 1.0$ and $\beta_2 = 0.0$. The mesh movement obviously improves the quality of the solution but the algorithm needs to be fine-tuned before it is of practical use. It should though be noted that the grid used here is very coarse: a finer mesh would be better able to pick out the features of the flow and supply enough nodes to provide considerably better resolution of the solution. A similar test case, but one which requires the use of the second derivative in the adaptation is given by defining the same initial conditions, except that $u = 1 - r$ for $r < 1$, where r is defined above. The solution is similarly improved (the peak value of u on the outflow plane is increased from 0.629 to 0.857), this time using $\beta_1 = 0.01$ and $\beta_2 = 1$.

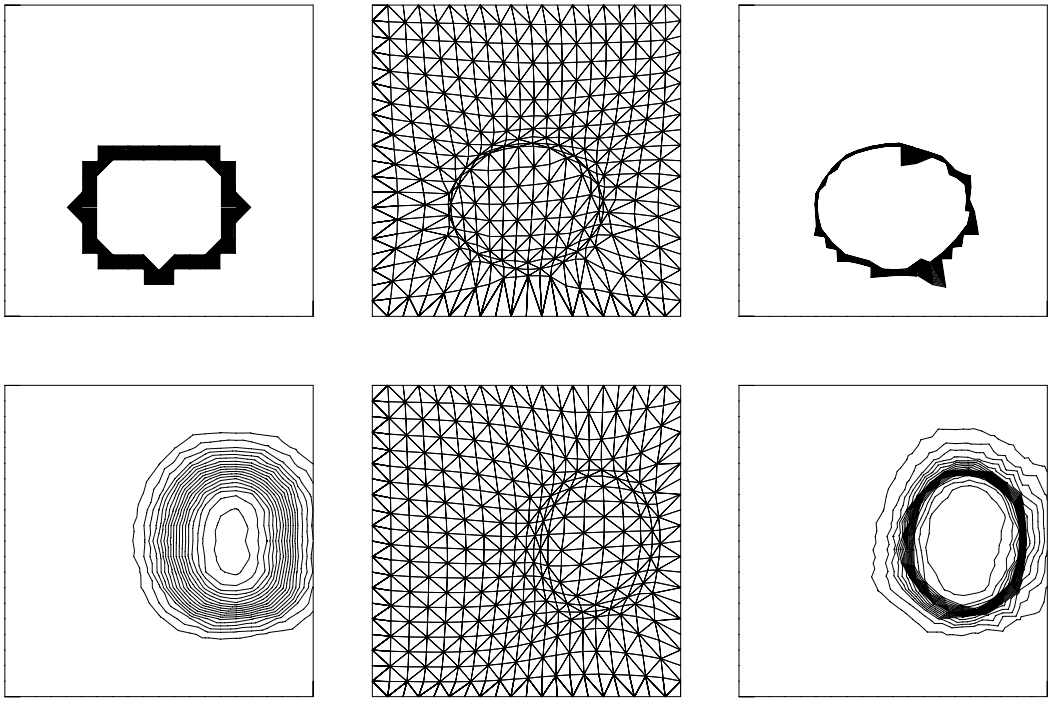

Figure 5.2: Grids and solutions for the advection of 'cylindrical' profile for the boundary planes at $z = 0$ (top) and $x = 0$ (bottom).

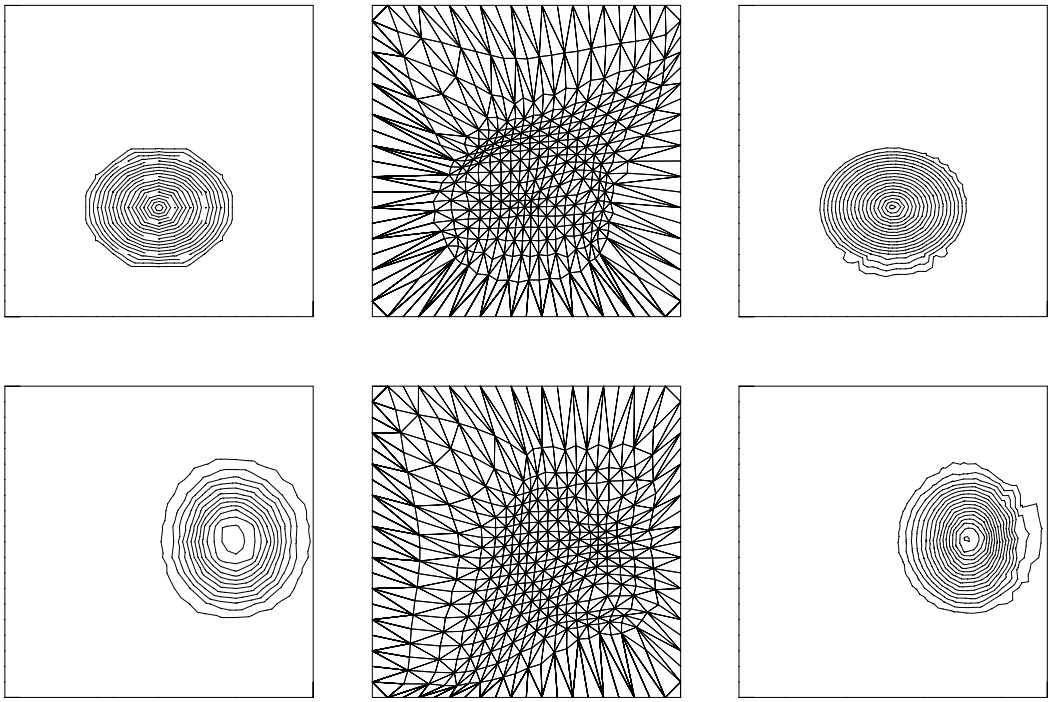

Figure 5.3: Grids and solutions for the advection of 'conical' profile for the boundary planes at $z = 0$ (top) and $x = 0$ (bottom).

6 Conclusions

The first steps towards four separate applications related to multidimensional upwind schemes have been presented here. Recently developed scalar fluctuation redistribution techniques for constructing high resolution monotone schemes are applied with some success to nonlinear systems of equations, but it is clear that more accurate and robust wave models will be necessary before the full benefit of these scalar techniques can be exploited. Source terms can be incorporated naturally into multidimensional upwind methods, and this 'upwind' discretisation is shown to improve significantly on the standard, pointwise approximations. The scalar schemes are then adapted crudely for use on spherical geometries. The scheme as it stands is consistent but not conservative: the latter property requiring a modified three-dimensional algorithm on a prismatic grid and additional constraints. The decomposition stage necessary for approximating the shallow water equations on the sphere represents an even bigger challenge, which may include the construction of three-dimensional wave models. Finally, a simple grid adaptation algorithm, which has been successfully applied in two dimensions is extended to the three-dimensional case and shown to work well on a simple test case.

7 Epilogue: the Current Situation

The family of multidimensional upwind schemes which has developed over the last fifteen years has now achieved a degree of success which has allowed them to be applied in practical situations where two-dimensional steady state flows are being approximated although up to now this has been predominantly in the field of aerodynamics. More recently, they have also been applied to problems in hydraulic engineering (the source terms which appear commonly in the modelling can be incorporated simply, but only at the expense of positivity). Note though that all of the applications presented here have been on triangular grids because, although the schemes can be extended to quadrilateral meshes, the linearisation procedure is less natural.

Furthermore, the methods have been shown to combine well with the standard

techniques for improving accuracy and efficiency, such as implicit time-stepping and grid adaptation through both refinement and movement. Viscous flow models have also been approximated (the Navier-Stokes equations) using these methods but, although the scalar fluctuation distribution technique can be extended to the advection-diffusion equation (by treating the viscous terms as sources), a Galerkin finite element discretisation of the viscous terms is often used.

Even now, though, these schemes have their limitations, the most noticeable being that the most accurate of the existing two-dimensional wave models have a singularity at a stagnation point. This can be dealt with satisfactorily in steady state calculations but remains a problem for time-dependent flows. Because of this, the recent advances in accurate fluctuation distribution schemes for time-dependent problems cannot be taken full advantage of: there is still much work to be done to construct appropriate decompositions for unsteady flows, and this may require an alternative approach to those used so far.

The situation with three-dimensional calculations is less well developed. The system decompositions have been applied with some success and the fluctuation distribution schemes readily generalise to the three-dimensional scalar advection equation (on tetrahedral meshes). It is also fairly simple to construct wave models along similar lines to those described here, but none has yet been proposed which incorporates the additional features apparent in the underlying three-dimensional models, *e.g.* bicharacteristics.

Acknowledgements

The author would like to thank Prof. M.J.Baines for his contributions to this work and the EPSRC for providing the funding for the author.

References

[1] M.J.Baines and M.E.Hubbard, 'Multidimensional upwinding with grid adaptation', in *Numerical Methods for Wave Propagation*, E.F.Toro and J.F.Clarke (Eds.), pp. 33–54, Kluwer Academic Publishers, 1998.

[2] M.E.Hubbard, 'Multidimensional upwinding and grid adaptation for conservation laws', PhD Thesis, The University of Reading, 1996.

[3] M.E.Hubbard and M.J.Baines, 'Conservative multidimensional upwinding for the steady two dimensional shallow water equations', *J. Comput. Phys.*, **138**:419–448, 1997.

[4] M.E.Hubbard and P.L.Roe, 'Compact high-resolution algorithms for time-dependent advection on unstructured grids', to appear, *Int. J. for Num. Methods in Fluids*, 1999.

[5] H.Deconinck, R.Struijs, G.Bourgois and P.L.Roe, 'High resolution shock capturing cell vertex advection schemes for unstructured grids', in *VKI LS 1994-05, Computational Fluid Dynamics*, 1994.

[6] H.Deconinck and B.Koren (editors), *Euler and Navier-Stokes solvers using multidimensional upwind schemes and multigrid acceleration*, Notes on Numerical Fluid Mechanics, volume 57, Vieweg, 1997.

[7] M.E.Hubbard, 'On the accuracy of one-dimensional models of steady converging/diverging open channel flows', Numerical Analysis Report 1/99, Department of Mathematics, University of Reading, 1999 (submitted to *Int. J. Numer. Methods Fluids*).

[8] M.E.Hubbard and M.J.Baines, 'Conservative multidimensional upwinding for the steady two dimensional shallow water equations', *J. Comput. Phys.*, **138**:419–448, 1997.

[9] P.Leyland and B.Khobalatte, 'The kinetic approach to multidimensional upwinding schemes', to appear, *7th Int. Conf. on Hyperbolic Problems*, Zurich, 1998.

[10] R.Löhner, K.Morgan, M.Vahdati, J.P.Boris and D.L.Book, 'FEM-FCT: combining unstructured grids with high resolution', *Communications in Applied Numerical Methods*, **4**:717–729, 1988.

[11] J.März, 'Improving time accuracy for residual distribution schemes', VKI PR 1996–17, von Karman Institute for Fluid Dynamics, 1996.

[12] L.M.Mesaros and P.L.Roe, 'Multidimensional fluctuation splitting schemes based on decomposition methods', AIAA Paper 95-1699, 1995.

[13] D.L.Williamson, J.B.Drake, J.J.Hack, R.Jakob and P.N.Swarztrauber, 'A standard test set for numerical approximations to the shallow water equations in spherical geometry', *J. Comput. Phys.*, **102**:211–224, 1992.